

# A depth-based method for functional time series forecasting

Antonio Elías\* and Raúl Jiménez†

Department of Statistics, Universidad Carlos III de Madrid

June 29, 2018

## Abstract

An approach is presented for making predictions about functional time series. The method is applied to data coming from periodically correlated processes and electricity demand, obtaining accurate point forecasts and narrow prediction bands that cover high proportions of the forecasted functional datum, for a given confidence level. The method is computationally efficient and substantially different to other functional time series methods, offering a new insight for the analysis of these data structures.

*Keywords:* functional time series, depth measures, central regions, forecasting, periodically correlated process, electricity demand.

---

\*Supported by the Spanish Ministerio de Educación, Cultura y Deporte under grant FPU15/00625.

†Partially supported by the Spanish Ministerio de Economía y Competitividad under grant ECO2015-66593-P.

# 1 Introduction

The concept of depth for functional data has received a great deal of attention since it was introduced by Fraiman and Muniz (2001). It has been used for several applications; including classification (López-Pintado and Romo, 2006; Cuevas et al., 2007; Cuesta-Albertos and Nieto-Reyes, 2008; Sguera et al., 2014; Hubert et al., 2017; Mosler and Mozharovskiy, 2017), outlier detection (Febrero et al., 2008; Ieva and Paganoni, 2013; Arribas-Gil and Romo, 2014; Chiou et al., 2014; Narisetty and Nair, 2015; Nagy et al., 2017), populations comparison (López-Pintado and Romo, 2009; López-Pintado et al., 2010; Nicholas et al., 2015), and clustering (Kwon and Ouyang, 2015; Singh et al., 2016; Tupper et al., 2017). Functional versions of boxplots and other graphical tools based on different depths have been also proposed for visualizing curves with the aim of discovering features from a sample that might not be apparent by using other methods (Hyndman and Shang, 2010; Sun and Genton, 2011; Serfling and Wijesuriya, 2017). These methods are based on the so called *central regions* that we combine here with some new ideas.

This paper addresses the problem of making predictions about functional time series. These data structures come from dividing an almost continuous time record into curves corresponding to natural consecutive periods, for example days. The forecasting problem in such as context has been an important field of research that has produced diverse seminal literature (Antoniadis et al., 2006; Hyndman and Shahid Ullah, 2007; Aneiros and Vieu, 2008; Hyndman and Booth, 2008; Aneiros et al., 2011). The prediction of a curve segment corresponding to an unobserved interval at the most recent period has been termed forecasting with dynamic updating (Shang and Hyndman, 2011). We use this context for presenting our approach. Unlike previous methods, we attempt to capture the morphology of the curve to predict without using any statistical model about temporal correlation among periods. We only suppose that the functional time series exhibits certain periodic structure. Then, past periods provide a library where we can search for some similarities with the most recent data.

The method is based on a selection of past curves that makes the segment of the most recent period a deep datum. We show that the bands delimited by the deepest curves from the selection cover high proportions of the curve segment to predict for a given confidence

level. We also provide a graphical tool for choosing how many curves to use, by taking into account the resulting band width and the proportion of time that the predicted curve will be into such band, for a given confidence level. From the entire selected curves, we also provide point forecast. The method is tested with simulated data and a real case study.

## 2 Description of the Method

Let  $Y$  be an almost continuous periodic time series of period  $p$ . Consider the curves  $y_1, y_2, \dots$  obtained by slicing  $Y$  into periods, this is

$$y_i(t) = Y(t + (i - 1)p), \quad 0 \leq t \leq p, \quad i = 1, 2, \dots \quad (1)$$

When  $y_1, \dots, y_n$  are observed on  $[0, p]$ , but  $y_{n+1}$  only on  $[0, q]$  (with  $q < p$ ), and we are interested in predicting  $y_{n+1}$  on  $(q, p]$ , we refer to  $\mathcal{Y}_n = \{y_1, \dots, y_n\}$  as the set of *sample curves* and to  $y_{n+1}$  as the *focal curve*.

### 2.1 Restricted and extended central regions

Let  $\mathcal{J}$  be a set with two or more sample curves and denote by  $\mathcal{J}^+$  the set obtained by adding the focal curve to  $\mathcal{J}$ .

For each  $y \in \mathcal{J}^+$ , consider the modified band depth of López-Pintado and Romo (2009) with bands formed by two curves

$$D_{[0,q]}(y, \mathcal{J}^+) = \frac{1}{2} \binom{m+1}{2}^{-1} \sum_{x,z \in \mathcal{J}^+} \lambda(\{t \in [0, q] : \min(x(t), z(t)) \leq y(t) \leq \max(x(t), z(t))\}),$$

$\lambda(\{t \in [0, q] : A(t)\})$  being the proportion of time that  $A(t)$  is true on  $[0, q]$ . Roughly,  $D_{[0,q]}(y, \mathcal{J}^+)$  is a measure of “centrality” or “outlyingness” of  $y$  with respect to  $\mathcal{J}^+$  on  $[0, q]$ .

Denote by  $\mathcal{J}_k$  the  $k$  deepest curves of  $\mathcal{J}$  according to  $D_{[0,q]}(\cdot, \mathcal{J}^+)$ . This is, the  $k$  curves of  $\mathcal{J}$  with largest  $D_{[0,q]}(\cdot, \mathcal{J}^+)$  values. Note that the focal curve does not belong to  $\mathcal{J}_k$  although it may be the deepest curve of  $\mathcal{J}^+$ . In this paper we consider the *Restricted Central Region* (RCR) on  $[0, q]$  delimited by the curves in  $\mathcal{J}_k$

$$R_k(\mathcal{J}) = \{(t, y(t)) : t \in [0, q], \min_{x \in \mathcal{J}_k} x(t) \leq y(t) \leq \max_{x \in \mathcal{J}_k} x(t)\} \quad (2)$$

and its *extension* on  $[q, p]$

$$\bar{R}_k(\mathcal{J}) = \{(t, y(t)) : t \in [q, p], \min_{x \in \mathcal{J}_k} x(t) \leq y(t) \leq \max_{x \in \mathcal{J}_k} x(t)\}. \quad (3)$$

We remark RCRs differ slightly from ordinary central regions based on band depth (Lopez-Pintado and Romo, 2007). These regions can reveal features such as magnitude and shape of the curves in play (Sun and Genton, 2011), particularly of the deep curves in  $\mathcal{J}^+$ . In principle, this utility is restricted to the interval where we measure the depth, this is  $[0, q]$ . However, if there is correlation between what is observed on  $[0, q]$  and what is observed on  $[q, p]$ , one expects that the extended RCRs have properties on  $[q, p]$  similar to those of RCR on  $[0, q]$ . This is a key idea in our approach. The correlation that we mention often arises from processes which are a mixture of randomness and periodicity, very common in stochastic modelling. This fact makes to our method a potential approach for a broad range of functional time series.

## 2.2 A depth-based algorithm for focal-curve enveloping

From the above, given a focal curve  $y_{n+1}$  and a set of sample curves  $\mathcal{Y}_n$ , we are interested on subsets of sample curves  $\mathcal{J}$  such that  $y_{n+1}$  is deep in  $\mathcal{J}^+$ , seeking that the shape and magnitude of  $y_{n+1}$  be captured by RCRs of  $\mathcal{J}$ . Of the  $2^n - 1 - n$  possible sets of sample curves, many of them may have RCRs which scarcely covers the focal curve, even if they are nearby (here we use Euclidean distance for measuring nearness but the method can be straightforwardly adapted to other distances). In general, the nearest curves to  $y_{n+1}$  may not envelope it. Conversely, many subsets may completely envelope the focal curve but with wide RCRs, whose boundaries are faraway from  $y_{n+1}$ . These regions do not provide useful information about the features of the focal curve.

To illustrate the argument above, consider the ten curves shown in Figure 1. Three different subsets  $\mathcal{J}$  of five blue curves are considered. The RCRs delimited by the two deepest curves of  $\mathcal{J}$  are shown in grey. At the left panel,  $\mathcal{J}$  is composed with the five nearest curves to the red one. Whereas at the central panel,  $\mathcal{J}$  consists of the five farthest curves. Our goal is to compute RCRs as the one shown in right panel. This is the tightest RCR that envelopes the focal curve.

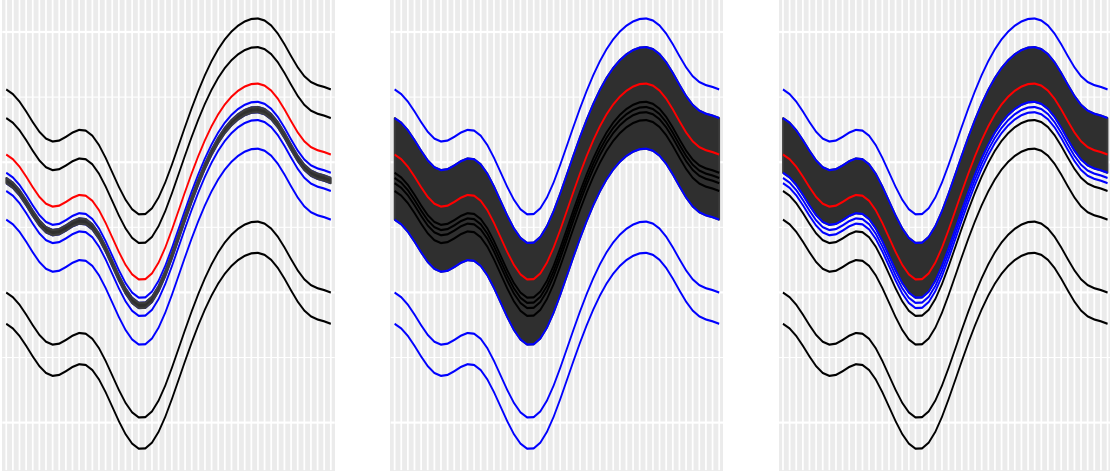


Figure 1: Three scenarios of bands (in gray) delimited by the two deepest curves of five blue curves. The blue curves correspond to (left panel) the five nearest lines to the red curve, (central panel) the five farthest curves, and (right panel) the set with tightest gray band that envelopes the focal curve.

We will address the problem by selecting curves *from*  $y_{n+1}$  *to outwards*, enveloping and making  $y_{n+1}$  a deep datum. For this, first we identify the set  $I_q \subset [0, q]$  where  $y_{n+1}$  is enveloped by the sample. This is

$$I_q = \{t \in [0, q] : \min_{y \in \mathcal{Y}_n} y(t) \leq y_{n+1}(t) \leq \max_{y \in \mathcal{Y}_n} y(t)\}. \quad (4)$$

We assume  $I_q$  is not empty and review curves, from the nearest curve to the farthest from  $y_{n+1}$ , to select those that contribute to cover  $y_{n+1}$  until this is completely enveloped on  $I_q$ . We gather these curves in  $\mathcal{J}$ . Next, we repeat the process but using the curves in  $\mathcal{Y}_n \setminus \mathcal{J}$  and save temporally the selected curves in  $\mathcal{N}$ . If the depth of  $y_{n+1}$  in  $\mathcal{J}^+ \cup \mathcal{N}$  does not decrease in relative terms respect to the depth in  $\mathcal{J}^+$  then we add  $\mathcal{N}$  to  $\mathcal{J}$ , otherwise we remove  $\mathcal{N}$  from  $\mathcal{Y}_n$ , and repeat the last process until there are not curves to select. We refer to the set of curves collected in  $\mathcal{J}$  as the *focal-curve envelope*. Properties of  $\mathcal{J}$  are: by construction, the band delimited by the curves in  $\mathcal{J}$  covers the focal curve on  $[0, q]$  as much as it is possible to do with the whole sample. Second, the nearest curves to  $y_{n+1}$  often belong to  $\mathcal{J}$ , although this is not usually a set of “ $k$ -nearest curves”. Finally, for the cases in which there exists a set of curves such that the focal curve is the deepest on  $[0, q]$ ,

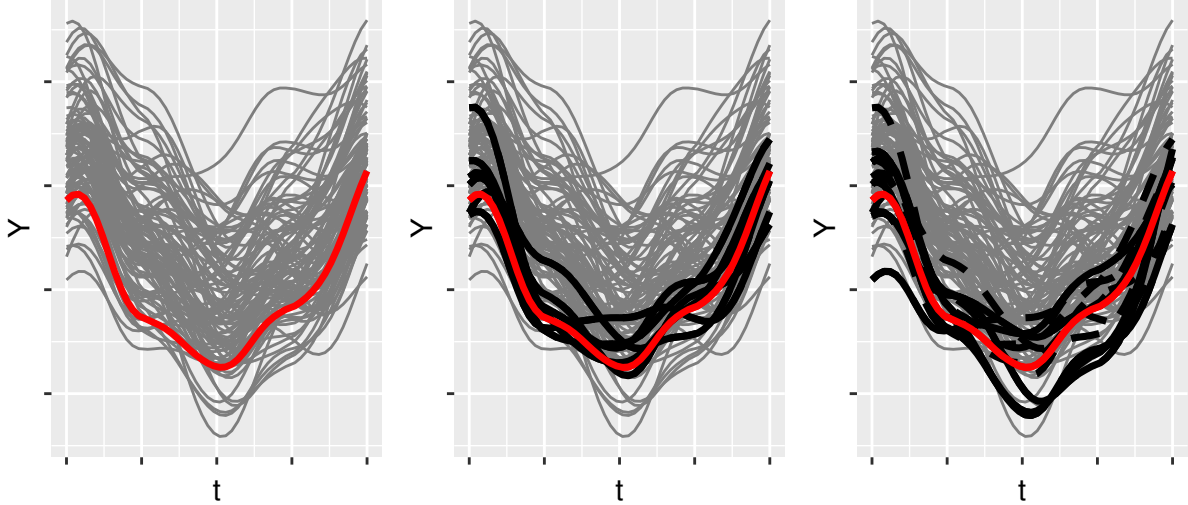


Figure 2: Left panel: sample curves (grey) and focal curve (red). Center panel: curves selected at the first iteration (black). Right panel: curves selected at the second/last iteration (black) and first iteration (dashed lines).

we have observed that  $y_{n+1}$  is also the deepest of  $\mathcal{J}^+$ . As illustration, Figure 2 shows first and last (second) iteration of the algorithm sketched above by considering 100 curves from a simulated functional time series. Note how the curves selected on the first iteration are near and cover the focal curve while the curves selected in the next iteration make it be the deepest curve of the envelope. To avoid ambiguities about how the algorithm works, we outline its steps in pseudocode (see Appendix).

### 2.3 Forecasting method

For band forecast, we consider extended RCRs of the focal-curve envelope  $\mathcal{J}$ , equation 3. Two statistics that either separately or combined are always considered for evaluating band forecast are: On one hand, the *coverage*; in our case, the proportion of time that the focal curve is in  $\bar{R}_k(\mathcal{J})$ . This is,

$$C_k(\mathcal{J}) = \lambda(\{t \in [q, p] : (t, y_{n+1}(t)) \in \bar{R}_k(\mathcal{J})\}). \quad (5)$$

On the other hand, the *band mean width*, that we standardize for comparing results on different functional time series. Namely,

$$W_k(\mathcal{J}) = \sum_{t \in [q,p]} \left( \max_{y \in \mathcal{J}_k} y(t) - \min_{y \in \mathcal{J}_k} y(t) \right) / \sum_{t \in [q,p]} \left( \max_{y \in \mathcal{Y}_n} y(t) - \min_{y \in \mathcal{Y}_n} y(t) \right). \quad (6)$$

This is a measure to assess how narrow is a prediction band relative to the band delimited by the whole sample. High coverage and small mean width are desirable to capture magnitude and shape of the focal curve. But both  $C_k$  and  $W_k$  are nondecreasing on  $k$ , therefore the selection of  $k$  involves a trade-off between coverage and mean width. The decision problem may be addressed by the graphical tool that we describe below.

Unlike mean width, coverage is random, it depends on the unobserved part of the focal curve. Hence, we consider expected coverage versus mean width for tuning  $k$ . Let  $\mu_k = \mathbb{E}[C_k(\mathcal{J})]$ . However, high expected coverage does not guarantee at all high coverage, not even high coverage with high probability. For this reason, for preventing poor coverages, we also consider a bottom threshold for the coverage with a  $(1 - \alpha) \times 100\%$  confidence level. Namely, the  $\alpha \times 100\%$  percentile of the probability distribution of  $C_k(\mathcal{J})$ , denoted here by  $c_k^\alpha$ . This is  $\mathbb{P}(C_k(\mathcal{J}) \leq c_k^\alpha) = \alpha$ . The idea, then, is to select  $k$  by taking into account  $\mu_k$ ,  $c_k^\alpha$  and  $W_k$ . In practice,  $\mu_k$  and  $c_k^\alpha$  must be estimated. For this, we consider the following plug-in approach:

Consider the  $m$  most recent periods previous to the focal one. Then consider the  $m$  envelopes  $\mathcal{J}(i)$ ,  $n - m + 1 \leq i \leq n$ , obtained by restricting data of  $y_i$  to  $[0, q]$  and computing the focal-curve envelope of  $y_i$  from the sample curves  $y_1, \dots, y_{i-1}$ . The average and the  $\alpha \times 100\%$  percentile of observed coverages  $C_k(\mathcal{J}(n - m + 1)), \dots, C_k(\mathcal{J}(n))$ , that we denoted by  $M_k$  and  $C_k^\alpha$ , are natural estimators of  $\mu_k$  and  $c_k^\alpha$ . The underlying idea is that under ergodic hypothesis about the functional time series, time averages should be similar to expected values. For this, we must assume that  $m$  and  $n - m$  are large. We explore this conjecture by simulation in next section. In particular, we provide statistical evidences for conjecturing  $M_k$  is an unbiased estimator of  $\mu_k$  and  $\mathbb{P}(C_k(\mathcal{J}) \geq C_k^\alpha) \geq 1 - \alpha$ .

Given a confidence level of  $(1 - \alpha) \times 100\%$ , we plot  $(W_k(\mathcal{J}), C_k^\alpha)$  and  $(W_k(\mathcal{J}), M_k)$  for several possible values of  $k$ . From this plot, the practitioner should select a  $k$  value that fits her/his preferences about mean width, expected and minimum coverage for a given confidence level. As illustration, we plot the resulting chart (left panel of Figure 3) by

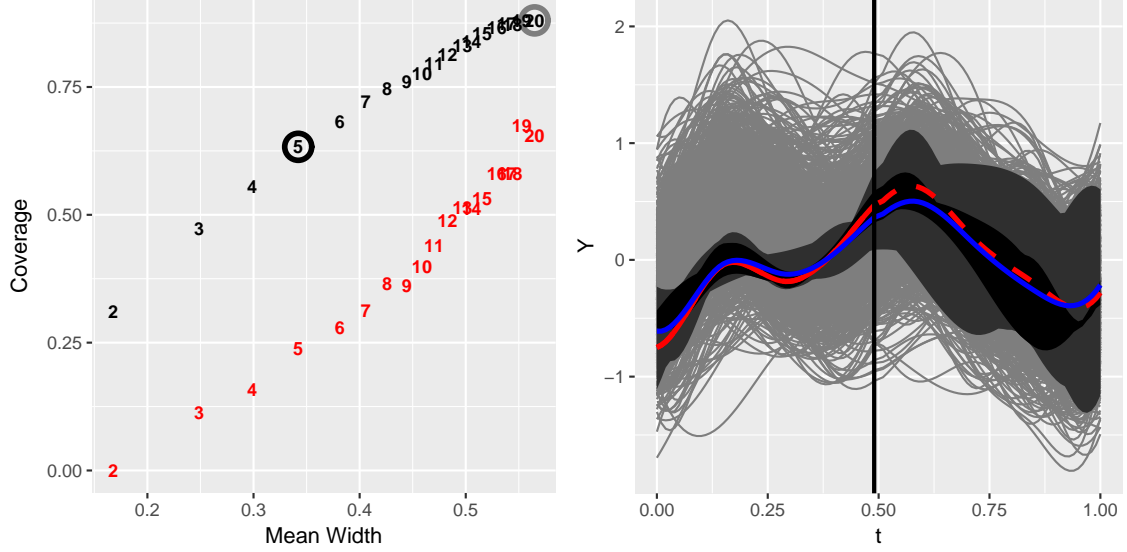


Figure 3: Left panel: Estimated expected coverage (black) for different  $k$ -values and corresponding lower bounds for a confidence level of 90% and mean widths. Right panel: Sample curves (grey), focal curve (red, observed part in solid line), restricted and extended central regions for  $k = 5$  and 20 (black and grey, respectively), and weighted functional mean of the focal-curve envelope (blue).

considering a simulated functional time series divided into  $n = 1000$  sample curves and a focal curve with  $p = 1$ ,  $q = 1/2$ ,  $m = 100$  and  $\alpha = 0.1$ . We also show (right panel) two RCRs and its extensions corresponding to  $k = 5$  and 20. From this plot we expect a coverage on the prediction interval above 62.5% for  $k = 5$  and 87.5% for  $k = 20$ . Also, with a confidence level of 90%, the coverage will be larger than 25% for  $k = 25$  and larger than 62.5% for  $k = 20$ .

For point forecast, we propose the weighted functional mean of the focal-curve envelope  $\mathcal{J}$ . This is,

$$\hat{y}_{n+1} = \sum_{y \in \mathcal{J}} w_y y, \quad \text{with } w_y = d(y, y_{n+1}) / \sum_{y \in \mathcal{J}} d(y, y_{n+1}), \quad (7)$$

$d(y, y_{n+1})$  being the Euclidean distance between  $y$  and  $y_{n+1}$  on  $[0, q]$ . Figure 3 (right panel) shows also point forecast for the example considered above.



### 3 Simulation Study

The class of the periodically correlated (PC) processes sets up a framework for modeling functional time series with complex periodic rhythm. They are processes whose mean and autocovariance function are periodic functions with same period. These models were introduced by Gladyshev (1961), since then they have been subject of study by several authors. The book of Harry L. Hurd (2007) presents the main theory as well as applications to meteorology, climate, communications, economics, and machine diagnostics.

We consider two stationary Gaussian processes that we combine to create a wide palette of PC processes. First, a Gaussian process  $X$  with zero mean and squared exponential autocovariance function

$$\text{Cov}(X(t), X(s)) = \sigma_X^2 \exp(-|t - s|^2 / 2l_X^2). \quad (8)$$

This is the default autocovariance function in Gaussian processes simulation (Rasmussen and Williams, 2005). The *lengthscale*  $l_X$  determines the length of the ‘wiggles’ in the trajectories. While  $\sigma_X$  determines the average distance of the trajectories away from zero. Second, a Gaussian process  $f$ , independent of  $X$ , with zero mean and periodic covariance function,

$$\text{Cov}(f(t), f(s)) = \sigma_f^2 \exp(-2 \sin^2(\pi|t - s|/p) / l_f^2). \quad (9)$$

The parameters  $l_f$  and  $\sigma_f$  determine lengthscale and average distance in the same way as in the squared exponential autocovariance function. We emphasize that the trajectories of  $f$  are periodic functions of period  $p$ .

We consider three types of seasonal signals:

$$Y_1(t) = f(t) + X(t), \quad Y_2(t) = f(t)X(t), \quad \text{and} \quad Y_3(t) = X(t + f(t)). \quad (10)$$

Sums of a seasonal and irregular component, as  $Y_1$ , have been widely used. In particular,  $Y_1$  is stationary, although its trajectories exhibit a periodic pattern of length  $p$ . However,  $Y_2$  and  $Y_3$  are non-stationary, they are periodically correlated with period  $p$ . If  $f$  were deterministic then  $Y_2$  would correspond to an *amplitude modulation* of a stationary process while  $Y_3$  to a *time-scale modulation*, frequently used signals in engineering. We randomize  $f$  by considering a Gaussian process with periodic covariance function for producing a

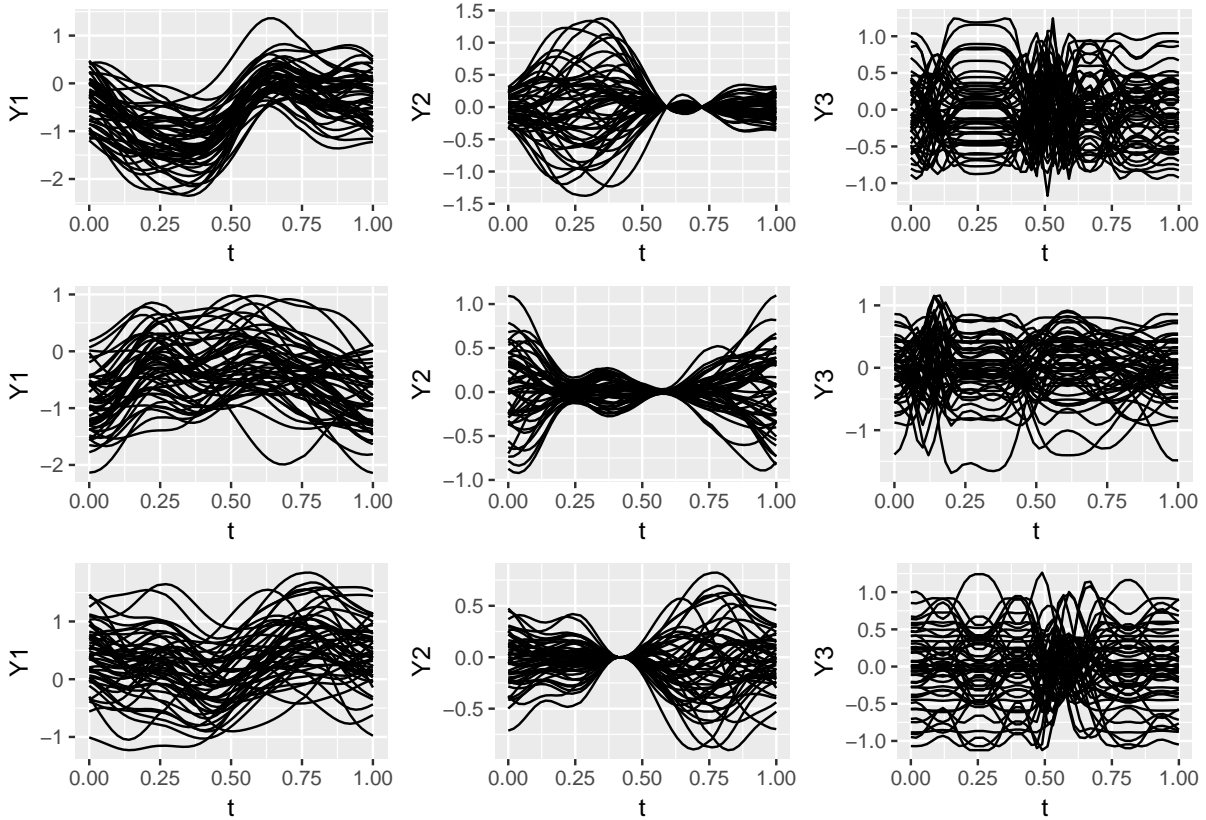


Figure 4: Examples of sample curves by slicing nine different trajectories of  $Y_1, Y_2$  and  $Y_3$ . The same observed periodic component from  $f$  is used by row and the same observed irregular trajectory from  $X$  is used by columns.

wide spectrum of sample curves. Figure 4 shows some examples of curves based on three observed patterns of  $f$ , with  $p = 1$ ,  $\sigma_X/\sigma_f = 1$  and  $l_X/l_f = 0.2$ .

### 3.1 Testing confidence level and expected coverage estimation

Before testing the goodness of our forecasting method, we test the two basic properties on which the practitioner bases her/his selection about which prediction band to use. They are,  $\mathbb{E}[M_k] = \mu_k$  and  $\mathbb{P}(C_k(\mathcal{J}) \geq C_k^\alpha) \geq 1 - \alpha$ . We address this problem by using Monte Carlo.

We simulated  $N$  independent trajectories of  $Y_i$ ,  $i = 1, 2$  and  $3$ . Each trajectory with 1001 periods, making  $n = 1000$  and reserving the last period as focal, with  $q = 1/2$ . We

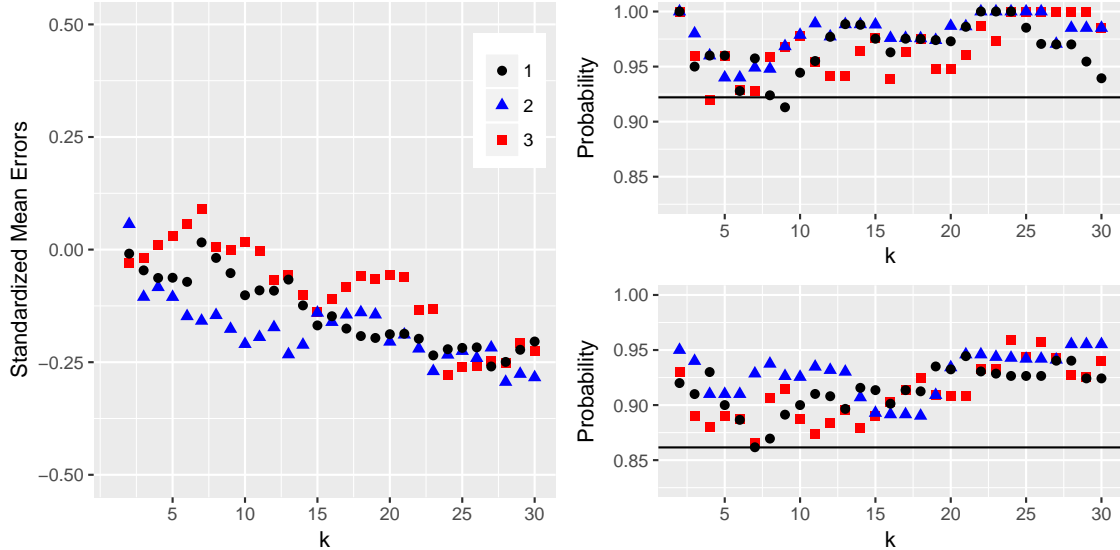


Figure 5: Left panel: standardized mean error of mean coverage estimators based on 100 independent trajectories of  $Y_i$ ,  $i = 1, 2$  and  $3$ . Right panel: Empirical probabilities that the observed coverage is greater than the bottom threshold proposed, for  $\alpha = 0.1$  (bottom) and  $\alpha = 0.05$  (top). Black lines delimit rejection regions at 95% confidence level for the hypothesis: the above probability is  $\geq$  than  $1 - \alpha$ .

fixed  $m = 100$  and observed  $M_k$  and  $C_k(\mathcal{J})$  for each trajectory, obtaining a paired random sample of size  $N$  of these statistics. Let  $d_j^k$  be the observed value of  $M_k - C_k(\mathcal{J})$  for the  $j$ th trajectory. Then, under the null hypothesis  $H_0 : \mathbb{E}[M_k] = \mu_k$ , the Central Limit Theorem implies that the standardized mean error  $\sqrt{N} \times \text{mean}(\{d_j^k\}_{j=1}^N) / \text{std}(\{d_j^k\}_{j=1}^N)$  is approximately standard normal when  $N$  is large. We computed this error for a wide range of  $k$  values and  $N = 100$  and observed all of them fallen between  $-0.3$  and  $+0.3$  (see left panel of Figure 5). Roughly, we have strong evidences against an alternative to  $H_0$ . A similar asymptotic argument based on the proportion of trajectories for which  $C_k(\mathcal{J}) \geq C_k^\alpha$  (i.e., the empirical probability) holds to reject the hypothesis  $\mathbb{P}(C_k(\mathcal{J}) \geq C_k^\alpha) < 1 - \alpha$ . Results for  $\alpha = 0.1$  and  $0.05$  are shown in right panel of Figure 5. In conclusion, the graphical tool for addressing the problem of choosing  $k$  works as we expected, at least for the considered PC processes.

## 3.2 Forecasting exercises with PC processes

We consider three scenarios for testing our forecasting method. First, a demanding practitioner with high coverage expectation (90%) and high threshold of minimum coverage (60%) without taking into account band mean width. Therefore, this practitioner looks for the smallest  $k$  such that  $M_k \geq 0.9$  and  $C_k^\alpha \geq 0.6$ . Although it is not the case for the simulations that we report below, we remark that it could happen that the focal-curve envelope has not enough sample curves for satisfying such condition on  $k$ . Second, a conservative practitioner with high coverage expectation but low threshold of minimum coverage (30%). This involves the smallest  $k$  such that  $M_k \geq 0.9$  and  $C_k^\alpha \geq 0.3$ . Finally, a conformist practitioner who is satisfied with  $M_k \geq 0.6$  and  $C_k^\alpha \geq 0.3$ .

In table 1, we observe the results when the three practitioner described above forecast the second half of the last 100 periods of one trajectory with 1,001 recorded periods of model  $Y_i$ ,  $i = 1, 2$  and 3. For these exercises we consider  $\alpha = 0.05$  and 0.10. The average of the selected  $k$  (that we denote by  $k^*$ ) across the 100 trials and the averages of the resulting coverage  $C_{k^*}(\mathcal{J})$  and mean width  $W_{k^*}(\mathcal{J})$  are reported in Table 1. It is also reported the empirical probability of  $C_{k^*}(\mathcal{J}) \geq 0.6$  for the first practitioner and the corresponding proportion of  $C_{k^*}(\mathcal{J}) \geq 0.3$  for the other two. Remarkably, the empirical probability fits the nominal one (0.90 and 0.95). This is, the proposed threshold of minimum coverage works for the two confidence levels considered. On the other hand, the observed coverage is larger in average than the expected coverage. This is because the selection rule of  $k$  typically involves larger  $k$ -values than those required to satisfy only a coverage-expectation condition. Finally, we remark that Practitioner 3 obtains high coverages and low mean width.

Boxplots of mean square errors of point forecast are plotting in Figure 6, showing accurate prediction for the three considered models of PC processes. As illustration, we also show prediction bands for the last period of each model in Figure 7.

	$\alpha = 0.05$				$\alpha = 0.10$			
$Y_1$								
Averages	$C_{k^*}(\mathcal{J})$	$W_{k^*}(\mathcal{J})$	Prob.	$k^*$	$C_{k^*}(\mathcal{J})$	$W_{k^*}(\mathcal{J})$	Prob.	$k^*$
Pract. 1	0.941	0.511	0.949	20.913	0.913	0.504	0.895	19.041
Pract. 2	0.938	0.509	0.966	20.588	0.876	0.468	0.895	14.570
Pract. 3	0.758	0.377	0.935	8.060	0.707	0.332	0.918	5.800
$Y_2$								
Averages	$C_{k^*}(\mathcal{J})$	$W_{k^*}(\mathcal{J})$	Prob.	$k^*$	$C_{k^*}(\mathcal{J})$	$W_{k^*}(\mathcal{J})$	Prob.	$k^*$
Pract. 1	0.942	0.529	0.952	21.256	0.929	0.509	0.926	18.878
Pract. 2	0.940	0.528	0.952	20.870	0.902	0.478	0.894	15.060
Pract. 3	0.807	0.388	0.948	8.170	0.731	0.329	0.910	5.780
$Y_3$								
Average	$C_{k^*}(\mathcal{J})$	$W_{k^*}(\mathcal{J})$	Prob.	$k^*$	$C_{k^*}(\mathcal{J})$	$W_{k^*}(\mathcal{J})$	Prob.	$k^*$
Pract. 1	0.915	0.461	0.958	19.263	0.915	0.455	0.900	17.700
Pract. 2	0.901	0.451	0.931	18.252	0.865	0.413	0.871	12.940
Pract. 3	0.742	0.326	0.927	7.170	0.662	0.289	0.860	5.370

Table 1: Three result sets obtained by predicting the second half of the last 100 periods of one trajectory with 1,001 periods. Each trajectory corresponds to one of the three PC processes denoted  $Y_1, Y_2$  and  $Y_3$ . Practitioner 1 select the smallest  $k$  such that  $M_k \geq 0.9$  and  $C_k^\alpha \geq 0.6$ . Practitioner 2, the smallest  $k$  such that  $M_k \geq 0.9$  but  $C_k^\alpha \geq 0.3$ . And. practitioner 3, the smallest  $k$  such that  $M_k \geq 0.6$  and  $C_k^\alpha \geq 0.3$ . Averages of observed coverage, mean width, empirical probability and selected  $k$  by the practitioner are grouped according to the confidence level used. We remark that the empirical probability fits the nominal probability 0.90 and 0.95, respectively.

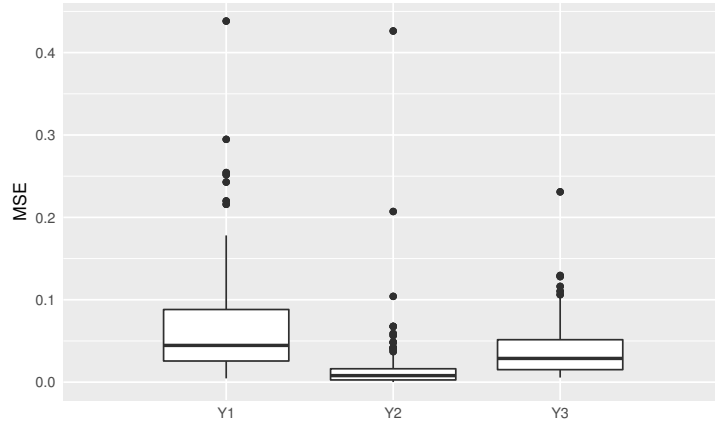


Figure 6: Mean Square Errors of proposed point prediction from the forecasting exercise based on trajectories of PC processes  $Y_1, Y_2$  and  $Y_3$ .

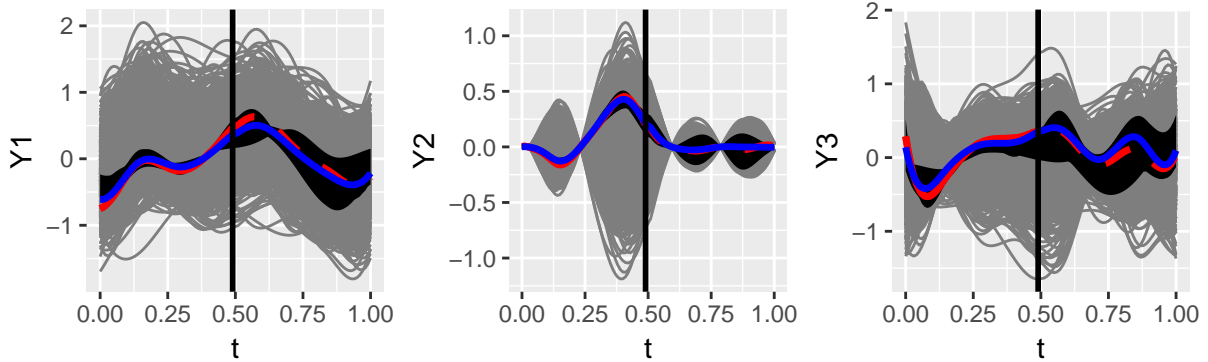


Figure 7: Left-half side of panels: focal curve (solid red line) and band (in black) based on the six deepest slices on  $[0, 1/2]$  provided by Algorithm 2. Right-half side of panels: extended extended bands and focal (dashed red line).

## 4 Case Study: Spanish electricity demand

Data concerning to the Spanish electricity demand is available at <http://www.ree.es/es/>, from where we obtained the demand in megawatts (MW) from January first 2014 to December 31st 2017 each 10 minutes. Thus, we consider the daily demand, 1461 curves in total. The demand varies significantly during the day, setting certain daily pattern that we can directly observe from simple plots showed below. Also it is reasonable to expect that the shape of the beginning of the day is correlated to the shape of the end, suggesting common characteristics with the PC processes discussed above. Of course, demand is more complicated than PC processes, we remark ruptures from working days to weekends or holidays, not to mention the difference among seasons. Otherwise, we could address the prediction problem estimating directly the PC structure.

Functional methods for electricity demand forecasting have been widely used (Vilar et al., 2012; Antoch et al., 2010; Paparoditis and Sapatinas, 2013; Cho et al., 2013; Shang, 2013; Aneiros et al., 2013). We recommend the paper of Aneiros et al. (2016), who also consider Spanish demand, for finding out more about functional data analysis for electricity forecasting. The methods developed by these authors are based on regression techniques that relies on the chronological order of the days, being able to provide accurate prediction for next-day electricity demand. Our functional data approach applied to this important problem is totally different and complementary. On one hand, we consider the practical case in which the demand of part of the day has been already observed and should be used for updating the prediction for the rest of the day. On the other hand, we review past days, without take care about how recent they are, to capture the phenomenology of the day to predict with the only goal of providing forecast bands that may be useful to anticipate critical scenarios.

Our forecasting exercise consisted in predicting half day of the 356 days of 2017. Boxplot and histogram of mean absolute percentage errors (MAPE) obtained are shown in Figure 8. Although they are different exercise, we remark that these MAPEs are smaller than those reported in the literature of functional methods for electricity demand forecasting. In any case, our errors are very small, concentrated below 2% and roughly they do not exceed 4%.

For testing the depth-based prediction bands, we consider again the three practitioner

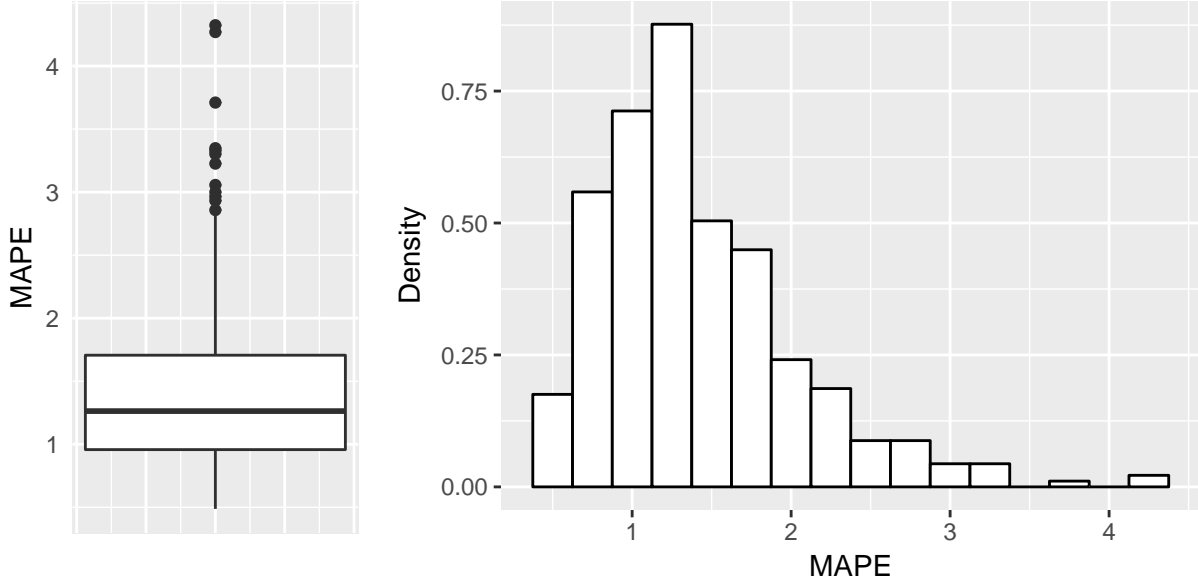


Figure 8: Boxplot and histogram of MAPEs obtained by predicting half day of Spanish electricity demand during 2017.

described on Section 3.2. The results obtained are shown in Table 2. They are even better than the results obtained for the PC processes. The prediction band of the three simulated practitioner are very narrow, remaining high coverages. To illustrate this case study, we show the plot from which the practitioner should select a  $k$  value by considering two days with a different patten of electricity demand.

As illustration, we show in top panel of Figure 9 the band corresponding to Tuesday, November 29th, 2016 by using Algorithm 1 and  $k = 10$ . Notably, all the curves used

	$\alpha = 0.05$				$\alpha = 0.10$			
Averages	$C_{k^*}(\mathcal{J})$	$W_{k^*}(\mathcal{J})$	Prob.	$k^*$	$C_{k^*}(\mathcal{J})$	$W_{k^*}(\mathcal{J})$	Prob.	$k^*$
Pract. 1	0.921	0.215	0.937	17.711	0.897	0.197	0.890	14.940
Pract. 2	0.921	0.215	0.937	17.711	0.877	0.185	0.911	13.134
Pract. 3	0.810	0.155	0.958	9.019	0.711	0.125	0.921	6.000

Table 2: Results obtained by the same practitioner profiles described on Table 1 by predicting half day of Spanish electricity demand during 2017.



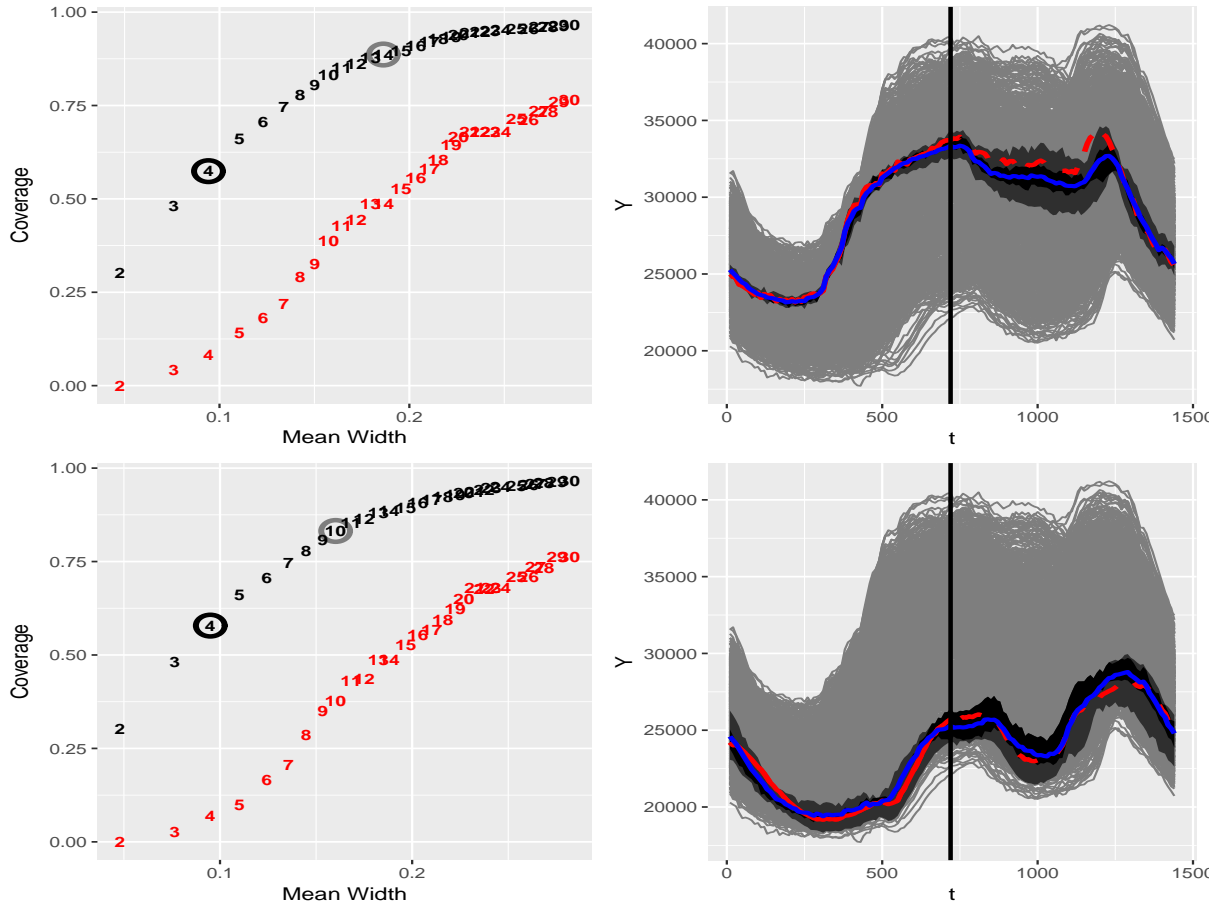


Figure 9: Two examples of predicting exercises for daily Spanish electricity demand. Focal curve (in red) corresponds to: Top panel, a standard working day (Tuesday, October 4th, 2017). Bottom panel, a Christmas day (December 25th, 2017).

to envelope the focal come from months between November and February, however they correspond to different working days and years.

## 5 Conclusions

Besides of providing point and band accurate forecast, the approach introduced here offers a new insight for functional time series forecasting. In contrast with other methods, our method is completely empirical driven without attending to any statistical model that could explain the mechanism of data generation.

The depth-based approach works with periodically correlated processes, that seem to give a wide pallet of test datasets for the functional time series analysis, and with case studies. Beyond prediction, the tools we have discussed reveal qualitative aspects of the data structure of electricity demand. For example, focal-curve curve envelopes link week-ends with holidays as well as atypical days with past outliers. Although these relations may appear somewhat naive, others could be not obvious. In general, envelopes can be useful for discovering common features among periods. The approach also introduce a tool for tuning coverage versus width in band forecasting. This allows to practitioners to compute tight predictions bands that may preserve the shape to the curve to predict by diminishing coverage and fixing confidence level. An alternative to other approaches in which the width band may be reduced only by losing confidence. The main limitation of our approach is it is designed to functional time series with periodic rhythm and without trend. If the effect of trend is negligible during a single period, one can subtract the functional mean to apply the method but there is no way of correcting the absence of periodic structure. Despite this, many real systems generate data which are mixtures of randomness and periodicity, making that the range of applications be wide.

To end, we remark about the computational efficiency of the method. The data sets we have considered in this work entail a big computational challenge; more than one thousand curves observed in more than one hundred points. These data quantities are not only hard to be processed quickly but even they suppose a problem of capability of being processed. In fact, regression-based methods require operations that may be intractable for sample sizes as we have considered. The methodology presented here is based on the Modified Band Depth and, as Sun et al. (2012) argue, this allows to rank million curves in only tens of seconds making our algorithm efficient even for large data sets than the considered in our experiments.

## References

Aneiros, G., Cao, R., and Vilar, J. M. (2011). Functional methods for time series prediction: a nonparametric approach. *J. Forecast.*, 30(4):377–392.

- Aneiros, G. and Vieu, P. (2008). Nonparametric time series prediction: A semi-functional partial linear modeling. *Journal of Multivariate Analysis*, 99(5):834–857.
- Aneiros, G., Vilar, J. M., Cao, R., and Muñoz, A. (2013). Functional prediction for the residual demand in electricity spot markets. *IEEE Transactions on Power Systems*, 28(4):4201–4208.
- Aneiros, G., Vilar, J. M., and Raña, P. (2016). Short-term forecast of daily curves of electricity demand and price. *International Journal of Electrical Power & Energy Systems*, 80:96–108.
- Antoch, J., Prchal, L., De Rosa, M. R., and Sarda, P. (2010). Electricity consumption prediction with functional linear regression using spline estimators. *Journal of Applied Statistics*, 37(12):2027–2041.
- Antoniadis, A., Paparoditis, E., and Sapatinas, T. (2006). A functional wavelet-kernel approach for time series prediction. *Journal of the Royal Statistical Society. Series B (Statistical Methodology)*, 68(5):837–857.
- Arribas-Gil, A. and Romo, J. (2014). Shape outlier detection and visualization for functional data: the outliergram. *Biostatistics*, 15(4):603–619.
- Chiou, J. M., Zhang, Y. C., Chen, W. H., and Chang, C. W. (2014). A functional data approach to missing value imputation and outlier detection for traffic flow data. *Transportmetrica B: Transport Dynamics*, 2(2):106–129.
- Cho, H., Goude, Y., Brossat, X., and Yao, Q. (2013). Modeling and forecasting daily electricity load curves: A hybrid approach. *Journal of the American Statistical Association*, 108(501):7–21.
- Cuesta-Albertos, J. and Nieto-Reyes, A. (2008). The random tukey depth. *Computational Statistics & Data Analysis*, 52(11):4979–4988.
- Cuevas, A., Febrero, M., and Fraiman, R. (2007). Robust estimation and classification for functional data via projection-based depth notions. *Computational Statistics*, 22(3):481–496.

- Febrero, M., Galeano, P., and González-Manteiga, W. (2008). Outlier detection in functional data by depth measures, with application to identify abnormal nox levels. *Environmetrics*, 19(4):331–345.
- Fraiman, R. and Muniz, G. (2001). Trimmed means for functional data. *Test*, 10(2):419–440.
- Gladyshev, E. (1961). Periodically correlated random sequences. *Sov. Math.*, 2:385–388.
- Harry L. Hurd, A. M. (2007). *Periodically Correlated Random Sequences: Spectral Theory and Practice*. Wiley Series in Probability and Statistics.
- Hubert, M., Rousseeuw, P., and Segaeert, P. (2017). Multivariate and functional classification using depth and distance. *Advances in Data Analysis and Classification*, 11(3):445–466.
- Hyndman, R. J. and Booth, H. (2008). Stochastic population forecasts using functional data models for mortality, fertility and migration. *International Journal of Forecasting*, 24(3):323–342.
- Hyndman, R. J. and Shahid Ullah, M. (2007). Robust forecasting of mortality and fertility rates: A functional data approach. *Journal of Computational & Graphical Statistics*, 51(10):4942–4956.
- Hyndman, R. J. and Shang, H. L. (2010). Rainbow plots, bagplots, and boxplots for functional data. *Journal of Computational & Graphical Statistics*, 19(1):29–45.
- Ieva, F. and Paganoni, A. M. (2013). Depth measures for multivariate functional data. *Communications in Statistics - Theory and Methods*, 42(7):1265–1276.
- Kwon, A. and Ouyang, M. (2015). Clustering of functional data by band depth. *Proceedings of the 9th EAI International Conference on Bio-inspired Information and Communications Technologies*, pages 510–515.
- López-Pintado, S. and Romo, J. (2006). Depth-based classification for functional data. In Regina Y. Liu, R. S. and Souvaine, D. L., editors, *Data Depth: Robust Multivariate*

*Analysis, Computational Geometry and Applications*, volume 72, page 103. AMS and DIMACS.

Lopez-Pintado, S. and Romo, J. (2007). Depth-based inference for functional data. *Computational Statistics & Data Analysis*, 51(10):4957–4968.

López-Pintado, S. and Romo, J. (2009). On the concept of depth for functional data. *Journal of the American Statistical Association*, 104(486):718–734.

López-Pintado, S., Romo, J., and Torrente, A. (2010). Robust depth-based tools for the analysis of gene expression data. *Biostatistics*, 11(2):254–264.

Mosler, K. and Mozharovskyi, P. (2017). Fast dd-classification of functional data. *Statistical Papers*, 58(4):1055–1089.

Nagy, S., Gijbels, I., and Hlubinka, D. (2017). Depth-based recognition of shape outlying functions. *Journal of Computational and Graphical Statistics*, 26(4):883–893.

Narisetty, N. N. and Nair, V. N. (2015). Extremal depth for functional data and applications. *Journal of the American Statistical Association*, 111(516):1705–1714.

Nicholas, T., Francesca, I., Rachele, B., and Anna, M. P. (2015). Use of depth measure for multivariate functional data in disease prediction: An application to electrocardiograph signals. *The International Journal of Biostatistics*, 11:189–201.

Paparoditis, E. and Sapatinas, T. (2013). Short-term load forecasting: The similar shape functional time-series predictor. *IEEE Transactions on Power Systems*, 28(4):3818–3825.

Rasmussen, C. E. and Williams, C. K. I. (2005). *Gaussian Processes for Machine Learning*. The MIT Press.

Serfling, R. and Wijesuriya, U. (2017). Depth-based nonparametric description of functional data, with emphasis on use of spatial depth. *Computational Statistics & Data Analysis*, 105:24–45.

Sguera, C., Galeano, P., and Lillo, R. (2014). Spatial depth-based classification for functional data. *TEST*, 23(4):725–750.

- Shang, H. L. (2013). Functional time series approach for forecasting very short-term electricity demand. *Journal of Applied Statistics*, 40(1):152–168.
- Shang, H. L. and Hyndman, R. J. (2011). Nonparametric time series forecasting with dynamic updating. *Math. Comput. Simul.*, 81(7):1310–1324.
- Singh, S. K., McMillan, H., Bádosy, A., and Fateh, C. (2016). Nonparametric catchment clustering using the data depth function. *Hydrological Sciences Journal*, 61(15):2649–2667.
- Sun, Y. and Genton, M. G. (2011). Functional boxplots. *Journal of Computational & Graphical Statistics*, 20(2):316–334.
- Sun, Y., Genton, M. G., and Nychka, D. C. (2012). Exact fast computation of band depth for large functional datasets: How quickly can one million curves be ranked? *Stat*, 1:68–74.
- Tupper, L. L., Matteson, D. S., Anderson, C. L., and Zephyr, L. (2017). Band depth clustering for nonstationary time series and wind speed behavior. *Technometrics*, 60(2):245–254.
- Vilar, J. M., Cao, R., and Aneiros, G. (2012). Forecasting next-day electricity demand and price using nonparametric functional methods. *International Journal of Electrical Power & Energy Systems*, 39(1):48–55.

## Appendix

---

**Algorithm 1** Input:  $\mathcal{Y}, y_{n+1}$ / Output:  $\mathcal{J}$

---

**Initialize**  $\mathcal{J} = \emptyset$

**while** size of  $\mathcal{Y} \setminus \mathcal{J} \geq 2$  **do**

Let  $y_{(k)}$  be the  $k$ th-nearest curve to  $y_{n+1}$  from  $\mathcal{Y} \setminus \mathcal{J}$ .

$\mathcal{N} = y_{(1)}$  and  $m = 0$

**for**  $k \geq 2$  **do**

$\mathcal{N}^k = \mathcal{N} \cup \{y_{(k)}\}$

$\lambda_k = \lambda(\{t \in [0, q] : \min_{y \in \mathcal{N}^k} y(t) \leq y_{n+1}(t) \leq \max_{y \in \mathcal{N}^k} y(t)\})$

**if**  $\lambda_k > m$  **then**

$\mathcal{N} = \mathcal{N}^k$  and  $m = \lambda_k$

**end if**

**end for**

Let  $p_0$  be the percentile of  $D_{[0,q]}(y_{n+1}, \mathcal{J}^+)$  in  $\{D_{[0,q]}(y, \mathcal{J}^+) : y \in \mathcal{J}^+\}$

Let  $p_1$  be the percentile of  $D_{[0,q]}(y_{n+1}, \mathcal{J}^+ \cup \mathcal{N})$  in  $\{D_{[0,q]}(y, \mathcal{J}^+ \cup \mathcal{N}) : y \in \mathcal{J}^+ \cup \mathcal{N}\}$

**if**  $p_1 \geq p_0$  **then**

$\mathcal{J} = \mathcal{J} \cup \mathcal{N}$

**else**

$\mathcal{Y} = \mathcal{Y} \setminus \mathcal{N}$

**end if**

**end while**

---